Animal (2019), **13:12,** pp 2830–2839 © The Animal Consortium 2019
doi:10.1017/S1751731119001319

animal

Evolution of pig intestinal stem cells from birth to weaning

N. Verdile[1], R. Mirmahmoudi[2], T. A. L. Brevini[3] and F. Gandolfi[1†]

[1]*Department of Agricultural and Environmental Sciences, University of Milan, Via Celoria 2, 20133 Milano, Italy;* [2]*Department of Animal Science, Faculty of Agriculture, University of Jiroft, P.O. Box 364, Jiroft, Iran;* [3]*Department of Health, Animal Science and Food Safety, University of Milan, Via Celoria 10, 20133 Milano, Italy*

(Received 12 September 2018; Accepted 6 May 2019; First published online 14 June 2019)

*Pig intestinal epithelium undergoes a complete renewal every 2 to 3 days that is driven by intestinal stem cells (**ISCs**) located at the crypt base in their niche. Intestinal stem cells generate a pool of highly proliferative transit-amplifying cells, which either migrate up the villus and differentiate into enterocytes and secretory cells or migrate towards the base of the crypt where they differentiate into Paneth cells that secrete antimicrobial peptides. The balance between ISCs' self-renewal and differentiation controls intestinal epithelial homeostasis; therefore, ISCs are essential for ensuring intestinal epithelial integrity. Detailed knowledge of these mechanisms in pig and other domestic species is very limited. Therefore, the aim of this work was to characterize ISC from birth to weaning. We analysed the duodenum, jejunum and colon of six piglets at birth, 6-day-old nursing piglets and 28-day-old weanlings, one week after weaning. We immunolocalized homeobox only protein$^+$ (**HOPX**) and sex-determining region Y-box 9$^+$ (**SOX9**) cells that identify quiescent and active ISC, respectively. The volume of ISCs was quantified with stereological methods and was compared to that of mitotic cells expressing proliferating cell nuclear antigen and apoptotic cells identified by the presence of cleaved caspase-3. Furthermore, we compared all these values with crypts and villi measurements and their ratio. Our results indicated that both quiescent and active ISCs are present in pig intestine from birth to weaning and are localized in the crypts of the small and large intestine. However, both markers were also observed along the villi and on the colon luminal epithelium, suggesting that at these stages, pig mucosa is still immature. Weaning induced a dramatic reduction of both HOPX$^+$ and SOX9$^+$ cells, but SOX9$^+$ cells underwent a significantly greater reduction in the small intestine than in the colon. This suggests that the two ISC types are differentially regulated along the intestinal tracts. Overall, the pig ISC complex has many similarities with its murine counterpart, but also has some differences. These include active ISC not showing the typical columnar base morphology as well as the absence of bona fide Paneth cells. This is the first description of ISC dynamics during pig's early life and provides useful reference data for future studies, aimed at targeting ISC for the development of efficient alternatives to in-feed antibiotics for preserving intestinal integrity.*

Keywords: epithelium, growth, intestine, renewal, repair

Implications

The pig industry requires that piglets are weaned as early as possible, causing distress and negative health repercussions that are mitigated by an extensive use of antibiotics. The risk of expanding antibiotic resistance led the European Union to ban the use of antibiotics as growth promoters in 2006. The healing process in response to epithelial injury is promoted by intestinal stem cells that, in pig, have been described and characterized only recently. The description of how intestinal stem cells evolve between birth and weaning is important for the development of innovative strategies to promote intestinal epithelium integrity without the use of antibiotics.

† E-mail: fulvio.gandolfi@unimi.it

Introduction

The intestinal epithelium displays the highest turnover of all solid organs, undergoing complete renewal every 2 to 3 days in pig (Gelberg, 2014). This is necessary because it must maintain a constant and effective barrier function in a harsh intestinal environment and, at the same time, ensure the absorption of all the necessary nutritional principles (Barker *et al.*, 2012).

The continuous replacement of the intestinal epithelium is driven by the ISCs located at the crypt base in their niche (Meran *et al.*, 2017). Intestinal stem cells generate a pool of highly proliferative transit-amplifying cells, which in most cases, migrate up the villus and differentiate into two major cell lineages: enterocytes for food absorption and secretory cells for mucus and hormone secretion (Meran *et al.*, 2017).

Paneth cells, on the contrary, are the only known cell type to migrate toward the base of the crypt where they secrete antimicrobial peptides and play an essential role in regulating ISC proliferation and differentiation (Clevers and Bevins, 2013).

The two ISC types coexist in the intestinal crypts, both in the small and large intestine (Li *et al.*, 2010). The best-characterized cells are the leucine-rich-repeat-containing G-protein-coupled receptor 5-expressing (**LGR5**$^{+}$) stem cells, which divide approximately every 24 h and, in mouse, are interspersed between the terminally differentiated Paneth cells. The LGR5^{+} cells are commonly named crypt base columnar (**CBC**) cells, as they are slender and reside at the bottom of the crypt (Clevers, 2013). The second type of stem cells are located at the +4 position of the intestinal crypt and are also known as label-retaining cells (**LRCs**), as they show long-term label retention upon irradiation damage and pulse labelling with bromodeoxyuridine and, differently from CBC cells, they are quiescent and act as a reserve population that can replace all intestinal cell lineages after tissue damage (Beumer and Clevers, 2016).

At birth, pigs have relatively mature muscular and nervous systems but their gastrointestinal (**GI**) tract is relatively immature, making them highly dependent on maternal milk for completing development and maturation (Sangild *et al.*, 2013). Naturally, this process would take a couple of months; however, current swine husbandry practices commonly anticipate weaning at 3 or 4 weeks of age (Davis *et al.*, 2006). This makes weaning the main critical period of the pig's production cycle because it is accompanied by multiple stressors that induce transient anorexia, intestinal inflammation and unbalanced gut microbiota. Such circumstances lead to GI infections that cause the death of around 17% of piglets born in Europe (Lallès *et al.*, 2007). For this reason, antimicrobials are still massively used in the swine industry for therapeutic purposes, but are also used as prophylactic or metaphylactic treatments to prevent GI infections (Gresse *et al.*, 2017), despite the ban on antibiotic growth promoters in the European Union since 2006. To comply with this ban, different feed ingredients, either alone or in combination with feed additives that are effective in reducing the incidence and severity of digestive problems, have been and are being actively developed (Pluske, 2013). In this regard, a better understanding of how ISCs regulate the rapid renewal of the intestinal epithelium would be useful for the development of innovative strategies to promote epithelium integrity without the use of antibiotics.

At present, little is known of the characteristics of pig ISC as most studies have been performed on mice and humans, but one study described in some detail the two stem cell populations present in the intestinal mucosa of this species (Gonzalez *et al.*, 2013). The authors provided a detailed description of several cell types in the pig intestinal mucosa, including stem cells and transit amplifying population, in 6- to 8-week-old individuals, but no quantitative assessment was provided.

The aim of this work was thus to describe the quantitative changes of the two main stem cell populations found in pig intestinal epithelium between birth and weaning. The changes were related to the villus and crypt measurements as well as to the amount of intestinal epithelial cell proliferation and apoptosis occurring during the early stages of life. These data will be useful to understand the physiological mechanisms that regulate intestinal epithelium growth during lactation, and its remodelling at the time of weaning.

Materials and methods

Animals and samples collection

A total of 18 healthy crossbred pigs derived from PIC (Large White × Landrace) females and Goland C21 males were obtained from a local farm. Six piglets were randomly selected from different litters, either immediately after parturition (unsuckling newborns), 6 days later (suckling piglets) or one week after weaning, at 28 days of age with body weight ranging from 7.6 to 8.4 kg. From day 10 after birth, while still with their own mother, piglets were exposed to a prestarter diet (Performer PLA, Ferrero Mangimi SpA, Farigliano, CN, Italy), based on cereals, milk powder, fish meal, vitamins and trace elements. At 21 days of age and at a weight ranging between 5.8 and 6.3 kg, piglets were separated from their mother, litters were mixed, and animals were fed *ad libitum* with the same prestarter diet. Animals were euthanized at the farm by intracardiac lethal injection under total anaesthesia according to current Italian regulation (law number 26/2014, attachment IV).

Immediately after sacrifice, in order to be consistent across individuals and across ages, unopened intestinal pieces of approximately 0.5 to 1 cm in length were taken from the central duodenum, jejunum and colon. Samples for histology were promptly fixed in 10% buffered formalin for 24 h at room temperature, dehydrated in graded alcohols, cleared with xylene and embedded in paraffin. Another adjoining fragment of approximately 5 cm was collected from each tract for measuring the organ volume as detailed below.

Histology and immunohistochemistry

After dewaxing and re-hydration, serial microtome sections (4 μm thick) of all samples were stained with haematoxylin–eosin (**HE**) to evaluate the structural aspects of the organs and measure villi and crypts. Other sections were stained with Periodic acid–Schiff to clearly identify goblet cells. Further sections were stained with Landrum's phloxine-tartrazine staining, specific for acidophilic secretory granules that characterize Paneth cells.

Images were acquired using a NanoZoomer S60 Digital slide scanner (C-13210-01, Hamamatsu) and observed at HAMAMATSU PHOTONICS ITALIA S.r.l., Arese, MI (Italy) continuous magnifications between 20 and 800×.

Villi height (from the apex of the villus to the villus–crypt junction), villi width (width of the villus at the middle of the villus height), crypt depth (from villus–crypt junction to the base of the crypt) and the villus:crypt ratio were measured on HE-stained sections with the NDP.view 2 software (Hamamatsu). The reported mean values were based on the measurements of 20 villi and 20 crypts per sample.

https://doi.org/10.1017/S1751731119001319 Published online by Cambridge University Press

We identified different cell populations by immunohistochemistry using antibodies specific for the following four antigens, as previously described (Gonzalez *et al.*, 2013). Homeobox only protein$^+$ (**HOPX**), a marker of +4 cells identifies the slow-cycling, LRC population distinct from the proliferating LGR5$^+$ cell population (Takeda *et al.*, 2011). Sex-determining region Y-box 9$^+$ (SOX9), a transcription factor expressed in mouse ISCs located at the bottom of the crypt and in the transient amplifying population (Shi *et al.*, 2013). Cleaved caspase-3 (**CASP3**), the most well-characterized effector caspase, is normally present in the cell as an inactive proenzyme. It is activated by a proteolytic process at conserved aspartic residues to produce the active enzyme that irreversibly triggers apoptosis (Parrish *et al.*, 2013). Proliferating cell nuclear antigen (**PCNA**), a specific marker of proliferating cells, has been well characterized also in pig intestine (Domeneghini *et al.*, 2004). The antibody details and working concentrations are summarized in Supplementary Table S1.

Antigen detection was performed by indirect immunohistochemistry using the avidin–biotin complex method (VECTASTAIN® Elite ABC, Vector Laboratories, USA) Burlingame, CA (USA) following the manufacturer instructions. Briefly, slides were brought to boiling point in 10 mM sodium citrate buffer and 0.05% Tween20 (pH 6) in a pressure cooker for 1 min for antigen retrieval. After cooling at room temperature for 15 min, sections were rinsed in phosphate-buffered saline (**PBS**, pH 7.4) and were then immersed in a freshly prepared 3% H_2O_2 solution in methanol for 15 min followed by HCl 0.3N in distilled water for 15 min to block the endogenous peroxidase activity. The aspecific binding was prevented by incubating sections using Normal Blocking Serum VECTASTAIN Elite ABC kit at room temperature for 30 min. Sections were incubated with one of the primary antibodies, listed in Supplementary Table S1, and diluted in 4% Bovine serum albumin (BSA) and PBS with 0.05% Tween20 for 1 h at room temperature in a humidified chamber. Sections were then incubated with appropriate biotinylated secondary antibody for 30 min at room temperature in a humidified chamber, followed by staining with the avidin–biotin complex (VECTASTAIN Elite ABC kit) for another 30 min. Finally, sections were incubated in 15% 3,3'-diaminobenzidine (DAB) peroxidase substrate solution until the desired stain intensity was obtained. Sections were briefly counterstained with Mayer's haematoxylin, dehydrated and permanently mounted with an aqueous mounting media (Biomount®, Bio-Optica, Milan, Italy). Secondary antibody controls were performed following the same staining protocol but omitting the primary antibody (Supplementary Figures S1 and S2).

Quantitative analysis

Systematic sampling and quantitative measurements were performed as described in detail previously (Albl *et al.*, 2016, Supplementary Material). Briefly, to determine the volume of each intestinal sample, we used the Archimedes' principle. We accurately determined the length of the intestinal samples collected at the time of sacrifice and performed the volume measurements using a 25 mL graduated cylinder, with a 0.5 mL scale filled with saline solution. The volume, expressed in µl, was then divided for the length of the intestinal segment, expressed in cm, to calculate the volume of 1 cm of each tract. This value was used to measure the volume of the cells positive to each antibody in each tract. We cut 4 µm sections perpendicular to the longitudinal axis of each organ (vertical sections) and collected at systematic random positions. Selected sections were stained either with HE or immunostained with specific antibodies as described above.

We used the HE-stained vertical sections to estimate the epithelium volume density (**Vv**) and the immunostained sections to estimate the Vv of cells positive for HOPX, SOX9, PCNA and CASP3. In accordance with the Delesse principle, a point-count stereologic grid with equally distant test points was used. The magnification range was chosen to allow the relevant portion of the intestinal wall to be contained in each field of vision (100× to 400×).

Vv was expressed as percentage and calculated as follows:

$$\mathrm{Vv}_{(\text{analyzed compartment, reference compartment})} = \left[\Sigma \mathrm{P}_{(\text{analyzed compartment})} / \Sigma \mathrm{P}_{(\text{reference compartment})}\right] \times 100$$

where $\Sigma P_{(\text{analyzed compartment})}$ is the number of points hitting the compartment under study and $\Sigma P_{(\text{reference compartment})}$ is the number of points hitting the relevant structure (i.e., intestinal wall or epithelium).

Furthermore, we used the Vv of HOPX$^+$, SOX9$^+$, PCNA$^+$ and cleaved CASP3$^+$cells to calculate their absolute volume (**Av**) as follows:

$$\begin{aligned}\text{Av of positive cells } (\mu\text{l/cm}) = {} & \mathrm{Vv}_{(\text{epithelium/intestinal wall})} \\ & \times \mathrm{Vv}_{(\text{positive cells/intestinal epithelium})} \\ & \times \text{volume of intestinal segment}\end{aligned}$$

Statistical analysis

The proportional values of each intestinal tract were analysed by Chi-square test across the three age groups (n=18). Quantitative data were expressed as mean ± SD. Results were analysed by using one-way ANOVA followed by all-pairwise multiple comparison test with Holm–Sidak method comparing values of each intestinal tract across the three age groups and comparing values of each age group across each section of the intestinal tract (n=18). Differences were considered statistically significant if $P<0.05$.

Results

Mucosa morphology

In the small intestine, villi height increased from birth to milk feeding and then decreased again at weaning. At the same time, villi's shape changed from digit to tongue-like. Crypts depth decreased at weaning and the villus:crypt ratio

https://doi.org/10.1017/S1751731119001319 Published online by Cambridge University Press

Table 1 *Small and large intestine histometry in the newborn (day 0), suckling (day 6) and weaned piglets (day 28)*

Stages of life[1]	Duodenum				Jejunum			Colon
	Villus length (µm)	Villus width (µm)	Crypts depth (µm)	Villus:crypt ratio	Villus length (µm)	Villus width (µm)	Crypts depth (µm)	Villus:crypt ratio	Crypts depth (µm)
Newborn	346.83^{a}±27.99	62.58^{a}±4.88	114.98^{a}±8.99	3.07^{a}±0.26	627.40^{a}±48.03	58.51^{a}±1.65	54.24^{a}±5.35	11.84^{a}±1.59	132.97^{a}±9.07
Suckling	568.35^{b}±50.13	88.11^{ab}±15.66	122.05^{a}±7.54	4.90^{b}±0.61	897.96^{b}±7.29	87.77^{a}±10.90	59.76^{a}±9.14	15.23^{b}±2.06	193.33^{b}±34.38
Weaned	278.10^{a}±72.44	110.19^{b}±18.15	192.08^{b}±25.60	1.54^{c}±0.22	201.76^{c}±18.13	73.39^{ab}±11.56	100.24^{b}±6.54	2.01^{c}±0.05	250.36^{c}±19.17

Values are expressed as means ± SD.
[a–c] Different superscripts in the same column indicate significant differences ($P<0.05$).
[1] $n=6$ for each stage of life.

increased from birth to milk feeding and sharply decreased at weaning. In the colon, crypt depth increased significantly at each step, from birth to weaning (Table 1). Furthermore, we observed that at birth and during milk feeding, there were more branched crypts than at weaning (Supplementary Figure S3).

At all ages, we did not observe the presence of cells showing the typical Paneth cell morphology, neither in the duodenum nor in the jejunum (Supplementary Figure S4). However, goblet cells were present, not only along the villi but also along the entire crypt depth (Supplementary Figure S5). In newborns' small and large intestine, we observed that the enterocyte nucleus was not in the commonly observed basal position, but was in the apical part of the cytoplasm (Supplementary Figure S6). The measure of enterocyte height indicated that this was not due to a different cell size or shape, but due to a true change of the nucleus position (Supplementary Table S2). We did not observe this peculiar nuclear location in any other age.

The quantitative assessment of the intestinal epithelium Vv measured the ratio between the intestinal surface and the wall thickness of each tract and the different stages of life. We observed that the ratio remained constant from birth to weaning in the small intestine but, at weaning, it was significantly reduced in the colon (Figure 1).

Homeobox only protein

We observed HOPX^{+} cells in the crypts of all tracts at all ages. Positive cells showed both nuclear and cytoplasmic location of the signal and were mostly located in the +4 to +6 positions from the bottom of the crypt, consistent with what has been previously observed in older pigs (Gonzalez *et al.*, 2013) and in mice (Figure 2b, d and f). However, a few HOPX^{+} cells were also observed along the villi in the duodenum and the luminal epithelium in the colon of newborn and suckling animals, whereas in the jejunum, these could also be found after weaning (Figure 2a, c and e).

Stereological quantification revealed that Av of HOPX^{+} cells increased significantly between birth and milk feeding in the small intestine and sharply decreased at the time of weaning in all intestinal tracts (Figure 3a). At birth and during milk feeding, HOPX^{+} cells were several times more abundant in the colon than in the small intestine. However, such a large significant difference largely disappeared at weaning (Supplementary Figure S7A).

Sex-determining region Y-box 9

We observed SOX9^{+} cells at the bottom of all crypts of all tracts at all ages. These cells were mostly round in shape and the SOX9 signal was in the nucleus. We did not determine SOX9^{+} elongated columnar cells, nor did we observe cells that could be recognized as typical Paneth cells with small apical granules (Figure 4a d and f); however, all cells at the bottom of the crypts were positive. SOX9^{+} cells were also observed in the upper parts of the crypts, along the villi and on the colon luminal surface. Typically, in these locations, the signal was also in the cytoplasm (Figure 4a, c and e).

https://doi.org/10.1017/S1751731119001319 Published online by Cambridge University Press

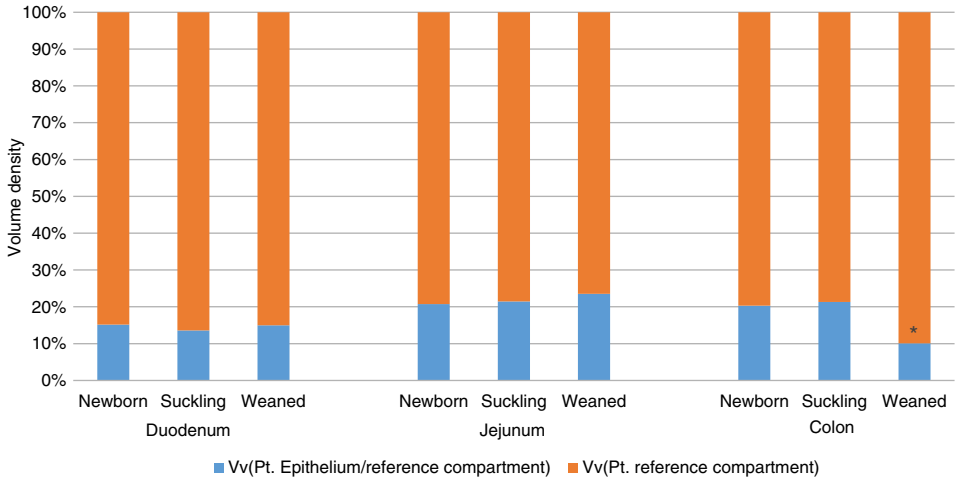

Figure 1 (colour online) Volume density (Vv) of piglets' intestinal epithelium in duodenum, jejunum and colon at different stages of life. Data are expressed as the percentage of the whole intestinal wall. *$P<0.05$. Pt: point.

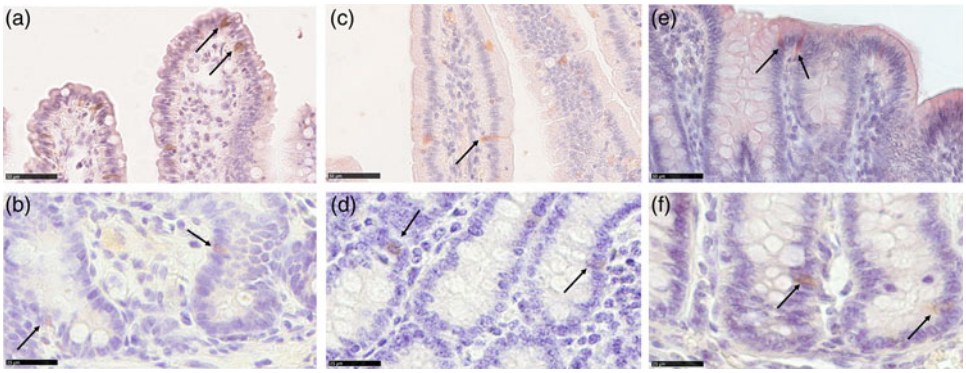

Figure 2 (colour online) Homeobox only protein signal identifies the quiescent stem cell population in piglets' small intestine and colon from birth to weaning. HOPX$^+$ cells (arrows) were observed in the +4 to +6 positions from the bottom of the crypt in the small and large intestine at all ages (b): jejunum weaned; (d): duodenum newborn; (f): colon suckling; scale bar=25 μm). Furthermore, HOPX$^+$ cells were also observed along the villi in the small intestine and on the colon luminal epithelium in newborn and suckling piglets. In the jejunum, HOPX positive cells were also found in weaned piglets (a): jejunum weaned; (c): duodenum suckling; (e): colon newborn; scale bar=50 μm). HOPX$^+$=Homeobox only protein.

Irrespectively of the location within the mucosa, the Av of SOX9$^+$ cells varied in the different tracts and along the development. In most cases, the signal increased between the birth and milk feeding and decreased at weaning within each tract (Figure 3b). However, at all ages, we measured a significantly larger SOX9$^+$cells volume in the colon than in the small intestine (Supplementary Figure S7B).

As expected, the ratio between SOX9$^+$ and HOPX$^+$ cells Av was always in favour of the former. This ratio significantly increased at weaning in the jejunum and colon but not in the duodenum (Figure 3c). However, the SOX9:HOPX volume ratio at birth was significantly lower than at weaning in the small intestine, but did not vary in the colon (Supplementary Figure S7C).

Proliferating cell nuclear antigen

We identified proliferating cells using PCNA immunostaining. In the crypts of all tracts at all ages, most, although not all, cells were proliferative. PCNA$^+$ cells were also present, although at low frequency, along the villi and on the luminal surface of the colon. In all locations, PCNA was specifically localized in the nucleus (Figure 5). Stereological quantification showed that the Av of proliferating cells statistically decreased at weaning, as expected (Figure 6a). Furthermore, the Av of proliferating cells was significantly larger in the colon than in the small intestine at birth and during lactation, whereas, at weaning, the Av dropped considerably, becoming almost similar in all tracts (Supplementary Figure S8A).

Cleaved caspase-3

We used an antibody specific for CASP3 cleaved at Asp-175, the biologically active form of CASP3, to identify cells actively undergoing the process of apoptosis. Cleaved caspase-3 was identified in cells at the apex of the villi and along the luminal colon epithelium, whereas no specific signal was observed in the crypts (Figure 7). Overall, the Av of apoptotic cells was small from birth to weaning and remained constant, except in the jejunum where we observed a gradual and significant increase in CASP3$^+$ cells along the growing phases we studied (Figure 6b). At all ages, apoptotic cells were rare;

https://doi.org/10.1017/S1751731119001319 Published online by Cambridge University Press

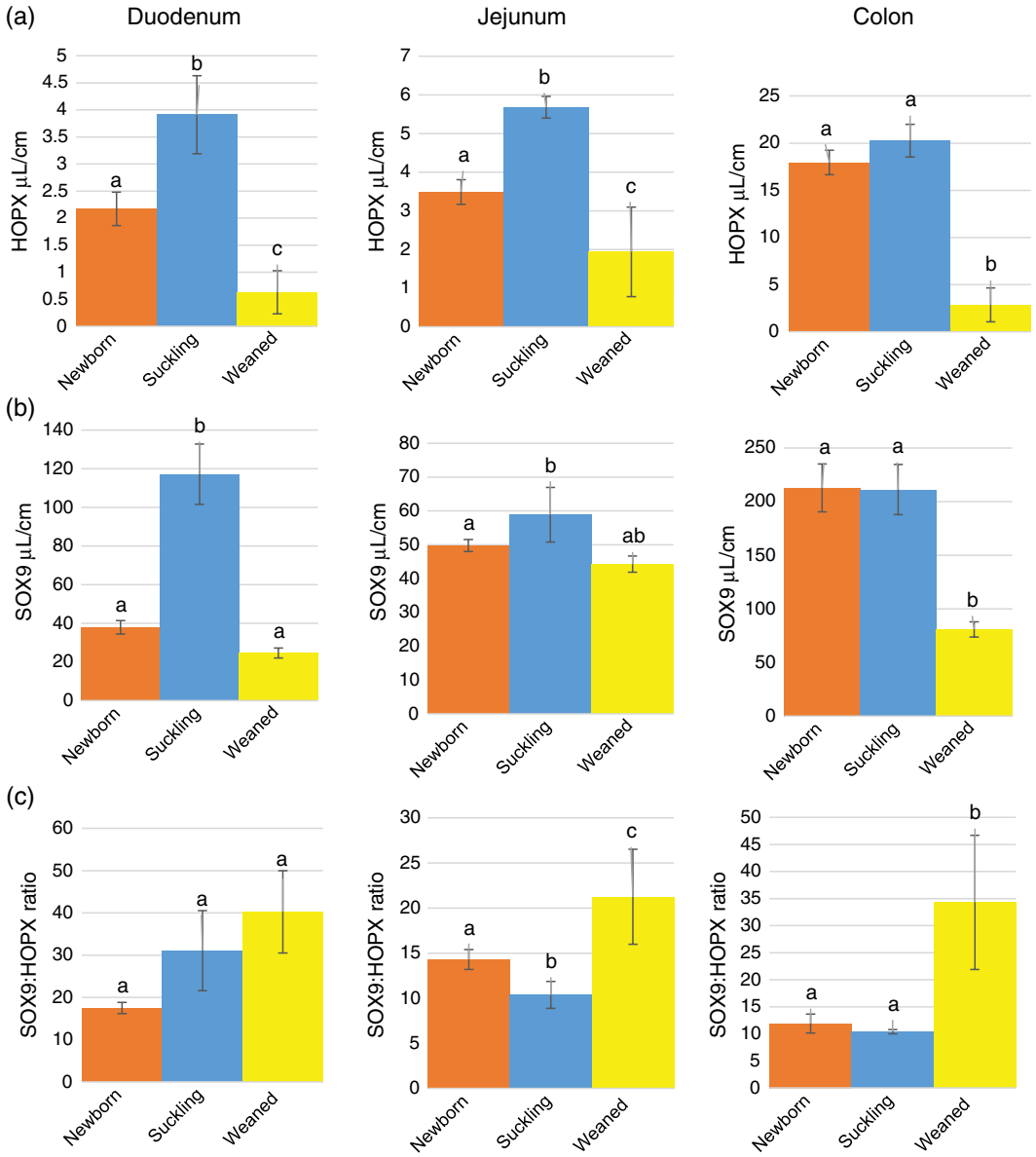

Figure 3 (colour online) Absolute volume of HOPX$^+$ (a) and SOX9$^+$ (sex-determining region Y-box 9) (b) cells and SOX9 : HOPX ratio (c) along the piglets' intestine. HOPX$^+$= homeobox only protein; SOX9$^+$=sex-determining region Y-box 9. $^{a–c}$Different superscripts within the same histogram indicate significant differences (P<0.05).

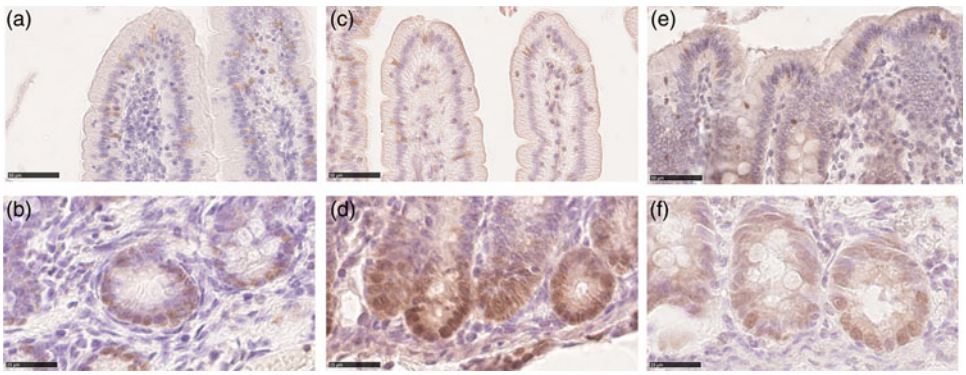

Figure 4 (colour online) Sex-determining region Y-box 9 immunostaining was localized in the nucleus of the cells within the crypt base of both the piglets' small intestine and colon at all ages (b): duodenum newborn; (d): jejunum suckling; (f): colon weaned; scale bar=25 µm). Both cytoplasmatic and nuclear SOX9 signals were observed along the villi in small intestine and colon luminal epithelium at all ages (a): duodenum weaned; (c): jejunum suckling; (e): colon newborn; scale bar=50 µm). SOX9=sex-determining region Y-box 9.

https://doi.org/10.1017/S1751731119001319 Published online by Cambridge University Press

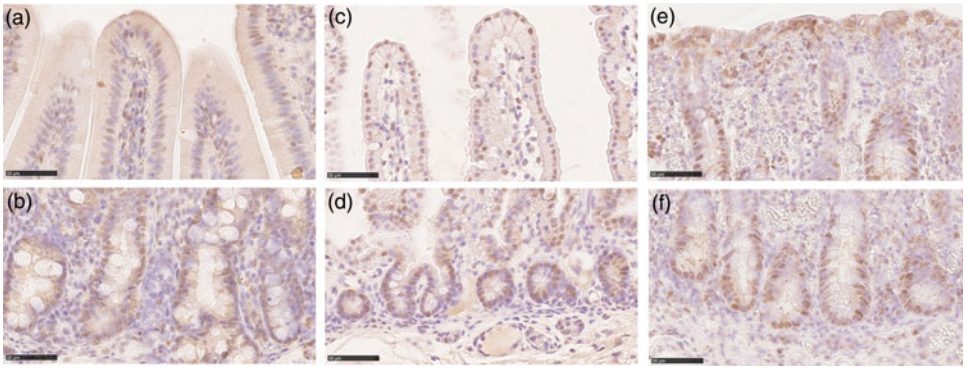

Figure 5 (colour online) Proliferating cell nuclear antigen immunolocalization was observed in the piglets' crypts in all tracts and at all ages (b): duodenum suckling; (d): jejunum newborn; (f): colon weaned; scale bar=50 μm). PCNA^{+} cells were also found along the villi in small intestine and colon luminal epithelium at all stages (a): duodenum suckling; (c): jejunum newborn; (e): colon weaned; scale bar=50 μm). PCNA = proliferating cell nuclear antigen.

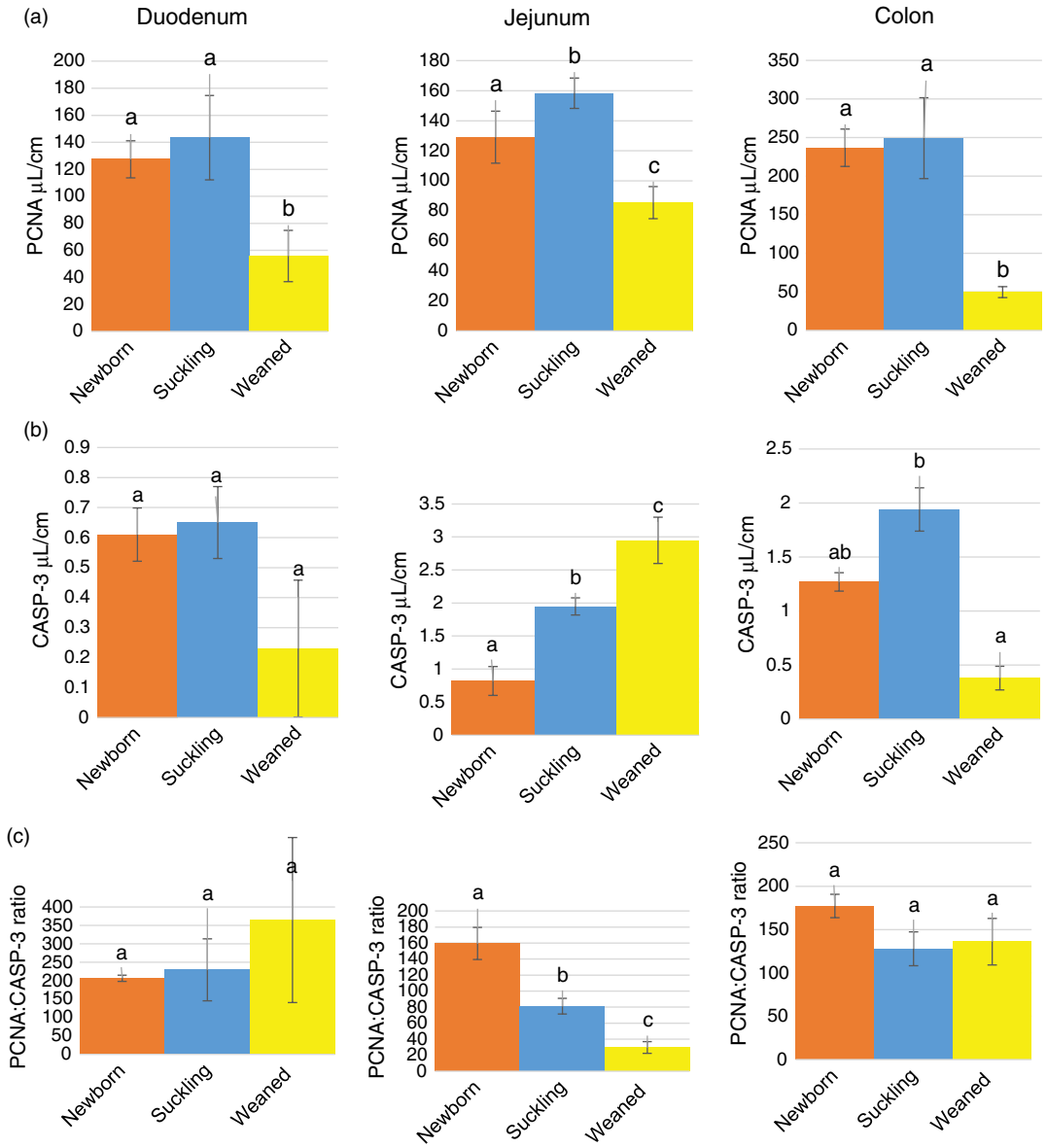

Figure 6 (colour online) Absolute volume of PCNA^{+} (proliferating cell nuclear antigen) (a) and CASP3^{+} (cleaved caspase-3) (b) cells and PCNA : CASP3 ratio (c) along the piglets' intestine. PCNA = proliferating cell nuclear antigen; CASP3=cleaved caspase-3. $^{a–c}$Different superscripts within the same histogram indicate significant differences (P<0.05).

https://doi.org/10.1017/S1751731119001319 Published online by Cambridge University Press

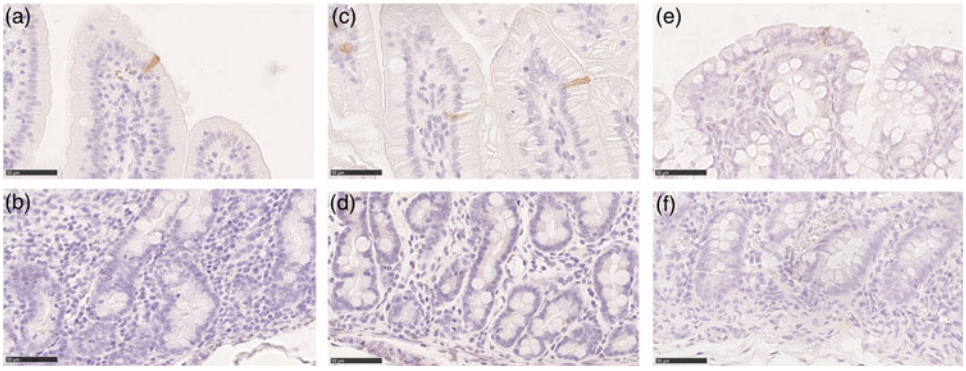

Figure 7 (colour online) Cleaved caspase-3 positive cells were found in the piglets' villi and on the colon luminal epithelium at all ages (a): duodenum weaned; (c): jejunum suckling; (e): colon newborn; scale bar=50 μm). No cleaved caspase-3^{+} cells were found in the crypts (b): duodenum weaned; (d): jejunum suckling; (f): colon newborn; scale bar=50 μm).

however, in most cases located in the colon at birth and during milk feeding, in this tract, apoptotic cells sharply decreased at weaning compared to that during milk feeding (Supplementary Figure S8B). The PCNA:CASP3 ratio showed a balance strongly in the favour of cell division from birth to weaning in the duodenum and colon, whereas in the jejunum, the ratio significantly decreased at each phase, reflecting the significant increase of apoptotic cells described above (Figure 6c). In fact, the jejunum at weaning was the only tract where apoptosis was in equilibrium with proliferation, as expected in an adult animal (Supplementary Figure S8C).

Discussion

In this study, we examined the evolution of ISCs from birth to weaning and correlated it with villi height and shape, crypt depth and villus:crypt ratio, the classical morphological features used to describe the tunica mucosa. We also applied a stereological method for the estimation of the intestinal wall volume in the different tracts, and the Vv of the tunica mucosa epithelial component of ISC as well as proliferating and apoptotic cells.

Our measurements of the tunica mucosa features are largely in agreement with data available in the literature (Godlewski *et al.*, 2005; Skrzypek *et al.*, 2018), confirming that the animals used in this study were healthy and normal. During the first 3 days after birth, the intestine doubles its weight and increases in length by 30% (Li *et al.*, 2014) and by the second week of life, the small intestine reaches its maximum length (Skrzypek *et al.*, 2018). According to a previous study, this results in an increase of the tunica mucosa Vv in the small intestine between foetal stage and birth, while it remains constant until weaning (Van Ginneken *et al.*, 2002). Our measurements of the mucosal epithelium Vv, including crypts, confirmed that it remained constant from birth to weaning in the small intestine. However, in the colon, we observed that mucosal epithelium Vv was significantly reduced at weaning, when we also observed a significant increase in crypt depth, that in mouse is considered a typical sign of inflammation (Erben *et al.*, 2014). The reduction of the colon epithelium Vv in combination with a significant increase in crypt depth suggests that, at this stage, colon epithelium is actively proliferating but it has been unable to fully recover from the regression induced by the weaning process. Indeed, the colon undergoes morphological changes around the time of weaning, similar to what has been described in the small intestine (Brunsgaard, 1998), whose morphological changes have been studied more intensively. In weaned pigs, we also observed a decrease in branched crypts, which is consistent with the notion that pig gut expansion occurs by a process of crypt multiplication in which crypts reproduce themselves by a fission mechanism (Brunsgaard, 1997).

Intestinal epithelial cell proliferation is very active and the whole population is entirely renewed every 2 to 3 days. Such a rapid turnover is driven by a small number of stem cells that are formed by two populations: the reserve ISCs, also known as +4 cells, characterized by a quiescent or slow cell cycle, under homeostatic conditions and the actively proliferating stem cells, also called CBC cells, which are major contributors to epithelial cells renewal.

The reserve ISCs do not possess a typical morphology and can be identified through a number of markers, among which HOPX has been validated in adult pigs (Gonzalez *et al.*, 2013). Our results indicate that HOPX^{+} cells are present in pig's intestinal mucosa from birth to weaning, in both the small and large intestinal tracts. The volume of positive cells, as expected, was quite low and these cells were located around the +4 position. We observed that their volume changed significantly throughout the first weeks of life, following the same pattern of proliferating cells. Although +4 cells are quiescent in the homeostatic conditions found in healthy adult animals, these variations are consistent both with the very rapid development of the whole intestine occurring in the first week of life and the well-known sharp decrease of epithelial proliferation associated with weaning (Heo *et al.*, 2013). We also observed that the volume of HOPX^{+} cells in the colon was significantly higher than in the small intestine at all stages, except at weaning. This is consistent

https://doi.org/10.1017/S1751731119001319 Published online by Cambridge University Press

with the previous observation that colon epithelium Vv is the only one to be affected by the weaning process.

In mouse, typical CBC cells are located at the bottom of the small intestine crypts between two Paneth cells, as well as in the colon crypts, and are characterized by LGR5 expression (Barker *et al.*, 2007). However, in pigs, this marker has proved to be ineffective, whereas SOX9 was localized in the regions where both stem and progenitor cells are expected (Gonzalez *et al.*, 2013). Unfortunately, this leaves only transmission electron microscopy as a way to identify columnar base cells and discriminate them from transient amplifying population (Gonzalez *et al.*, 2013), thus making accurate quantification very difficult.

We also observed that, while all cells at the bottom of the crypts are SOX9 positive (Figure 4), not all of them express PCNA (Figure 5). This suggests that at the bottom of the crypts, there are cells with a labelling pattern ($SOX9^+$ and $PCNA^-$) compatible with the properties of Paneth cells (Bastide *et al.*, 2007; Mori-Akiyama *et al.*, 2007). However, the lack of the typical acidophilic apical granules prevents their description as *bona fidae* Paneth cells rather we are observing Paneth-like cells, as also previously suggested by Gonzalez *et al.* (2013). Irrespectively, these cells are likely to have functional relevance in the light of the recent data indicating that Paneth cells do not only have a well-characterized bacteriostatic function, but also play a fundamental role in the regulation of CBC cells (Clevers and Bevins, 2013).

Interestingly, cells located at the bottom of the crypts showed a distinct nuclear location of the SOX9 signal, whereas, along the villi and on the colon luminal epithelium, the signal was diffused into the cytoplasm as well. This could be explained by the observation that SOX9 is expressed either at low or high steady-state levels in SOX9-enhanced green fluorescent protein ($SOX9^{EGFP}$) transgenic mice (Formeister *et al.*, 2009). In these animals, high levels of $SOX9^{EGFP}$ were accompanied by the expression of chromogranin A and substance P but not by the proliferation marker Ki67, suggesting that SOX9 could also be expressed by post-mitotic enteroendocrine cells.

The SOX9:HOPX ratio was significantly higher in jejunum and colon at weaning, indicating that pig ISCs are likely to follow a functional model where the quiescent, reserve population of stem cells ($HOPX^+$) is specifically activated upon injury and might convert into progeny or active stem cells, which are both $SOX9^+$ (Beumer and Clevers, 2016). Overall, our results confirm and expand the findings of Gonzalez *et al.* (2013) who described $HOPX^+$ and $SOX9^+$ cells in the same locations in animals a few weeks older than those we examined. More recently, LGR5 and BMI1, another marker for +4 cells, have both been cloned in pig (Li *et al.*, 2014, 2018), opening the way for the generation of pig-specific reagents.

The presence of the activated form of caspase (CASP3) was very rare at all ages and in all intestinal tracts that we examined, indicating a very low rate of apoptosis. This is consistent with the high mitosis or apoptosis ratio, typical of the growing phase of these animals also described by previous studies (Widdowson *et al.*, 1976; Skrzypek *et al.*, 2005). In our samples, apoptotic cells were visible only at the apex of the villi or in the colon luminal epithelium. This is in contrast with previous observations in neonatal piglets, which described apoptotic cells along the entire length of the villi, including the lower half and noted that dying cells were eliminated into the lumen as single cells or groups of cells (Godlewski *et al.*, 2005). A possible explanation for such discrepancy is that we used an antibody specific for the cleaved and active form of caspase, whereas the previous studies used an antibody that was described as specific for caspase-3 and may have also recognized the uncleaved precursor. This would have led to the staining of cells still not actively undergoing the process of apoptosis. However, the presence of a small number of CASP3 positive cells was also described in older (6 to 8 weeks) pigs (Gonzalez *et al.*, 2013). This suggests that caspase-3, an essential element of both intrinsic and extrinsic apoptotic pathways, may be activated after initiation of cell shedding (anoikis), consistent with findings in mice that caspase-3 was undetectable until after other features of cell shedding were evident (Marchiando *et al.*, 2011).

Conclusions

We can conclude that the ISC structure described in mouse largely overlaps with our current observations in pig, with some limitations including the lack of an adequate antibody for LGR5 that prevents an unequivocal identification of the so-called active stem cells. However, the recent observation that LGR5 and BMI1 are overexpressed in a pig intestinal cell line (Li *et al.*, 2018) further supports the idea that pig intestinal epithelium proliferation is regulated through mechanisms similar to that of the mouse.

The lack of some typical morphological characteristics associated with *bona fidae* Paneth cells still makes their indisputable identification problematic, even if functionally equivalent cells are likely to be present.

The accurate cell quantification suggests that, at weaning, $HOPX^+$ cells may convert into $SOX9^+$ cells; however, this hypothesis cannot be tested without performing lineage tracing experiments that are not currently possible in pigs. Nevertheless, it will be interesting to verify if similar observations will also be reported in other stressful circumstances like intestinal infections.

Overall, these results are useful to better understand the cellular mechanisms regulating cell proliferation at weaning or other stress and how to possibly harness them to preserve epithelial integrity.

Acknowledgements

This work was supported by DISAA development funds and by the University of Jiroft grant. The authors are grateful to Andrea Minardi and Matteo Ghiringhelli for their support

https://doi.org/10.1017/S1751731119001319 Published online by Cambridge University Press

with animal sampling and to Silvia Arba and Marco Ferrari for their help with immunolabelling.

T. A. L. Brevini, 0000-0002-0428-3621
F. Gandolfi, 0000-0002-3246-2985

Declaration of interest

The authors declare no conflict of interest

Ethics statement

The experimental procedures were approved by the University of Milan Ethics Committee (Decision n. OPBA_82_2017).

Software and data repository resources

None of the data was deposited in an official repository.

Supplementary material

To view supplementary material for this article, please visit https://doi.org/10.1017/S1751731119001319

References

Albl B, Haesner S, Braun-Reichhart C, Streckel E, Renner S, Seeliger F, Wolf E, Wanke R and Blutke A 2016. Tissue sampling guides for porcine biomedical models. Toxicologic Pathology 44, 414–420.

Barker N, Van Es JH, Kuipers J, Kujala P, Van Den Born M, Cozijnsen M, Haegebarth A, Korving J, Begthel H, Peters PJ and Clevers H 2007. Identification of stem cells in small intestine and colon by marker gene Lgr5. Nature 449, 1003–1007.

Barker N, van Oudenaarden A, Clevers H, van Oudenaarden A and Clevers H 2012. Identifying the stem cell of the intestinal crypt: strategies and pitfalls. Cell Stem Cells 11, 452–460.

Bastide P, Darido C, Pannequin J, Kist R, Robine S, Marty-Double C, Bibeau F, Scherer G, Joubert D, Hollande F, Blache P and Jay P 2007. Sox9 regulates cell proliferation and is required for Paneth cell differentiation in the intestinal epithelium. The Journal of Cell Biology 178, 635–648.

Beumer J and Clevers H 2016. Regulation and plasticity of intestinal stem cells during homeostasis and regeneration. Development 143, 3639–3649.

Brunsgaard G 1997. Morphological characteristics, epithelial cell proliferation, and crypt fission in cecum and colon of growing pigs. Digestive diseases and sciences 42, 2384–2393.

Brunsgaard G 1998. Effects of cereal type and feed particle size on morphological characteristics, epithelial cell proliferation, and lectin binding patterns in the large intestine of pigs. Journal of Animal Science 76, 2787–2798.

Clevers H 2013. The intestinal crypt, a prototype stem cell compartment. Cell 154, 274–284.

Clevers HC and Bevins CL 2013. Paneth cells: maestros of the small intestinal crypts. Annual Review of Physiology 75, 289–311.

Davis ME, Sears SC, Apple JK, Maxwell C V. and Johnson ZB 2006. Effect of weaning age and commingling after the nursery phase of pigs in a wean-to-finish facility on growth, and humoral and behavioral indicators of well-being. Journal of Animal Science 84, 743–756.

Domeneghini C, Di Giancamillo A, Savoini G, Paratte R, Bontempo V and Dell'Orto V 2004. Structural patterns of swine ileal mucosa following L-glutamine and nucleotide administration during the weaning period. An histochemical and histometrical study. Histology and Histopathology 19, 49–58.

Erben U, Loddenkemper C, Doerfel K, Spieckermann S, Haller D, Heimesaat MM, Zeitz M, Siegmund B and Kühl AA 2014. A guide to histomorphological evaluation of intestinal inflammation in mouse models. International Journal of Clinical and Experimental Pathology 7, 4557–4576.

Formeister EJ, Sionas AL, Lorance DK, Barkley CL, Lee GH and Magness ST 2009. Distinct SOX9 levels differentially mark stem/progenitor populations and enteroendocrine cells of the small intestine epithelium. AJP: Gastrointestinal and Liver Physiology 296, G1108–G1118.

Gelberg HB 2014. Comparative anatomy, physiology, and mechanisms of disease production of the esophagus, stomach, and small intestine. Toxicologic Pathology 42, 54–66.

Godlewski MM, Słupecka M, Woliński J, Skrzypek T, Skrzypek H, Motyl T and Zabielski R 2005. Into the unknown – the death pathways in the neonatal gut epithelium. Journal of Physiology and Pharmacology: An Official Journal of the Polish Physiological Society 56 Suppl 3, 7–24.

Gonzalez LM, Williamson I, Piedrahita JA, Blikslager AT and Magness ST 2013. Cell lineage identification and stem cell culture in a porcine model for the study of intestinal epithelial regeneration. PLoS ONE 8, e66465.

Gresse R, Chaucheyras-Durand F, Fleury MA, Van de Wiele T, Forano E and Blanquet-Diot S 2017. Gut microbiota dysbiosis in postweaning piglets: understanding the keys to health. Trends in Microbiology 25, 851–873.

Heo JM, Opapeju FO, Pluske JR, Kim JC, Hampson DJ and Nyachoti CM 2013. Gastrointestinal health and function in weaned pigs: a review of feeding strategies to control post-weaning diarrhoea without using in-feed antimicrobial compounds. Journal of Animal Physiology and Animal Nutrition 97, 207–237.

Lallès J-P, Bosi P, Smidt H and Stokes CR 2007. Nutritional management of gut health in pigs around weaning. Proceedings of the Nutrition Society 66, 260–268.

Li CM, Yan HC, Fu HL, Xu GF and Wang XQ 2014. Molecular cloning, sequence analysis, and function of the intestinal epithelial stem cell marker Bmi1 in pig intestinal epithelial cells. Journal of Animal Science 92, 85–94.

Li L, Clevers H, LeBoeuf MR, Wang Q, Lu MM, Epstein JA, Li N and Clevers H 2010. Coexistence of quiescent and active adult stem cells in mammals. Science 327, 542–545.

Li X-G, Wang Z, Chen R-Q, Fu H-L, Gao C-Q, Yan H-C, Xing G-X and Wang X-Q 2018. LGR5 and BMI1 increase pig intestinal epithelial cell proliferation by stimulating WNT/β-Catenin signaling. International Journal of Molecular Sciences 19, 1036.

Marchiando AM, Shen L, Graham WV, Edelblum KL, Duckworth CA, Guan Y, Montrose MH, Turner JR and Watson AJM 2011. The epithelial barrier is maintained by in vivo tight junction expansion during pathologic intestinal epithelial shedding. Gastroenterology 140, 1208–1218.e2.

Meran L, Baulies A and Li VSW 2017. Intestinal stem cell niche: the extracellular matrix and cellular components. Stem Cells International 2017, 1–11.

Mori-Akiyama Y, van den Born M, van Es JH, Hamilton SR, Adams HP, Zhang J, Clevers H and de Crombrugghe B 2007. SOX9 is required for the differentiation of Paneth cells in the intestinal epithelium. Gastroenterology 133, 539–546.

Parrish AB, Freel CD and Kornbluth S 2013. Cellular mechanisms controlling caspase activation and function. Cold Spring Harbor Perspectives in Biology 5, a008672.

Pluske JR 2013. Feed- and feed additives-related aspects of gut health and development in weanling pigs. Journal of Animal Science and Biotechnology 4, 1.

Sangild PT, Thymann T, Schmidt M, Stoll B, Burrin DG and Buddington RK 2013. Invited review: the preterm pig as a model in pediatric gastroenterology. Journal of Animal Science 91, 4713–4729.

Shi Z, Chiang C-I, Mistretta T-A, Major A and Mori-Akiyama Y 2013. SOX9 directly regulates IGFBP-4 in the intestinal epithelium. American Journal of Physiology. Gastrointestinal and Liver Physiology 305, G74–G83.

Skrzypek T, Valverde Piedra JL, Skrzypek H, Woliński J, Kazimierczak W, Szymańczyk S, Pawłowska M and Zabielski R 2005. Light and scanning electron microscopy evaluation of the postnatal small intestinal mucosa development in pigs. Journal of Physiology and Pharmacology: An Official Journal of the Polish Physiological Society 56 Suppl 3, 71–87.

Skrzypek TH, Kazimierczak W, Skrzypek H, Valverde Piedra JL, Godlewski MM and Zabielski R 2018. Mechanisms involved in the development of the small intestine mucosal layer in postnatal piglets. Journal of Physiology and Pharmacology: An Official Journal of the Polish Physiological Society 69, 127–138.

Takeda N, Jain R, LeBoeuf MR, Wang Q, Lu MM and Epstein JA 2011. Interconversion between intestinal stem cell populations in distinct niches. Science 334, 1420–1424.

Van Ginneken C, Van Meir F, Sys S and Weyns A 2002. Stereologic characteristics of pig small intestine during normal development. Digestive Diseases and Sciences 47, 868–878.

Widdowson EM, Colombo VE and Artavanis CA 1976. Changes in the organs of pigs in response to feeding for the first 24 h after birth. Neonatology 28, 272–281.